CONTROLLING DIFFUSIVE TRANSPORT IN CONFINED GEOMETRIES*

P.S. Burada

Max-Planck Institut für Physik Komplexer Systeme
Nöthnitzer Str. 38, 01187 Dresden, Germany

G. Schmid, Y. Li, P. Hänggi

Institut für Physik, Universität Augsburg
Universitätsstr. 1, 86135 Augsburg, Germany

(Received January 25, 2010)

We analyze the diffusive transport of Brownian particles in narrow channels with periodically varying cross-section. The geometrical confinements lead to entropic barriers, the particle have to overcome in order to proceed in transport direction. The transport characteristics exhibit peculiar behaviors which are in contrast to what is observed for the transport in potentials with purely energetic barriers. By adjusting the geometric parameters of the channel one can effectively tune the transport and diffusion properties. A prominent example is the maximized enhancement of diffusion for particular channel parameters. The understanding of the role of channel-shape provides the possibility for a design of stylized channels wherein the quality of the transport can be efficiently optimized.

PACS numbers: 05.60.Cd, 05.40.Jc, 02.50.Ey

1. Introduction

Diffusion process in narrow confined systems exhibits peculiar properties which are radically different from what we generally observe in free systems, *i.e.*, in absence of any geometrical restrictions [1]. If we consider a Brownian particle which is moving in a potential energy landscape or in a confined geometry where the geometrical confinement may regulate or control the diffusion process, the diffusion varies significantly from the free case [2–4].

* Presented at the XXII Marian Smoluchowski Symposium on Statistical Physics, Zakopane, Poland, September 12–17, 2009.

Depending on the conditions imposed, the effective diffusion coefficient can be larger or smaller than the bulk diffusion coefficient. Brownian particles when moving in a confined geometry undergo a constrained diffusive motion. This feature of constrained motion is ubiquitous in ion channels, nanopores, zeolites, and for processes occurring at sub-cellular level [4–16]. The uneven shape of these structures regulates the transport of particles yielding important effects exhibiting peculiar properties [4, 13–15]. The results have implications in processes such as catalysis, osmosis and particle separation [5–8, 11, 12] and on the noise-induced transport in periodic potential landscapes that lack reflection symmetry, such as ratchet systems [17–20].

Nowadays, artificial, *i.e.*, synthetic, nanopores are available [7, 21, 22] to characterize the transport characteristics of ionic species like K^+, Na^+, Cl^- [7, 16] and of macro molecules, like DNA or RNA [22–26]. With latest technology, these synthetic nanopores can be made upon choice, allowing for effective control of the diameter and the shape of the nanoporous structure [7, 21, 22]. In recent years, it has been of great interest to reveal the sequence and structural analysis of DNA and RNA molecules by passing them through nanopores [23–28]. When a double stranded DNA molecule passes through the charged nanopore, each base pair exhibits its own distinct electronic signature because each base pair is structurally and chemically different. While present conventional methods to find out this sequence would take several months and are expensive, one could find the sequence of a human genome in a matter of hours at a potentially low cost using this new technology. In addition, charging of the inner tube walls could lead to rectification of the motion of ions [7, 16, 29].

It has been found that the separation of macromolecule fragments and ions in narrow channels [13–15, 22, 24] is largely influenced by their shape alone. The characteristic behavior of ionic currents of these molecules or individual species can effectively change if the pore diameter changes [24, 26, 30–32]. The subject of this paper is to systematically illustrate the role of the channel properties on the transport characteristics for Brownian particles passing through the channels.

The paper is organized in the following way. In Sec. 2 we introduce the model system, the dynamics and discuss the complications involved in solving the full problem. The reduction of dimensionality, or in other words the simplification, and an analytical treatment of the problem is discussed in Sec. 3. In Sec. 4 we introduce the simulation techniques to solve the full problem numerically. The main findings on the transport characteristics are discussed in Sec. 5. In Sec. 6 we present the main conclusions.

2. Modeling

We investigate the transport of Brownian particles through straight channels with periodically varying cross-section. In the following, we mainly focus on 2D-channels (see Fig. 1), although a very similar line of reasoning could be applied for pore structures in 3D. For a model system we consider a channel structure whose shape is defined by the periodic boundary function $\omega(x)$ with the periodicity L, *i.e.* $\omega(x+L) = \omega(x)$. The diffusive motion of the Brownian particle is then confined by the upper boundary $\omega(x)$ and the lower boundary $-\omega(x)$. In particular, we choose:

$$\omega(x) = A \sin\left(2\pi \frac{x}{L}\right) + B\,, \tag{1}$$

with the two channel parameters A and B, and where the function $\omega(x)$ is thought to be the first terms of the Fourier series of a more complex boundary function. Due to the symmetry with respect to the x-axis the boundary function could be given in terms of the maximum half-width of the channel $w_{\max} = (A+B)$ and the aspect ratio of minimum and maximum width $\varepsilon = (B-A)/(B+A)$, *i.e.*

$$\omega(x) = \frac{w_{\max}}{2}\,(1-\varepsilon)\,\left\{\sin\left(2\pi \frac{x}{L}\right) + \frac{1+\varepsilon}{1-\varepsilon}\right\}\,. \tag{2}$$

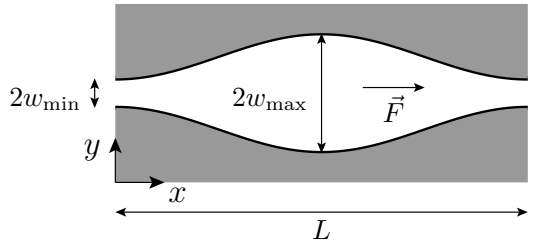

Fig. 1. Schematic representation of a single cell of a channel with the periodicity L, bottleneck half-width $w_{\min}$ and maximal half-width $w_{\max}$. The shape of the structure is defined by Eq. (2). The constant, applied bias F is acting only along the length of the channel.

Transport through the considered confined geometry may be caused by different particle concentrations maintained at the ends of the channel, or by the application of external forces acting on the particles. Here we will exclusively consider the case of force driven transport. The external driving force is denoted by $\vec{F} = F\vec{e}_x$ which points into the direction of the channel axis. Then the dynamics of a suspended Brownian particle is described by means of the Langevin equation which reads in the over damped limit [33]:

$$\gamma \frac{d\vec{x}}{dt} = \vec{F} + \sqrt{\gamma\, k_{\mathrm{B}}\, T}\, \vec{\xi}(t)\,, \tag{3}$$

where t is time, $\vec{x}$ the position vector of the particle, γ its friction coefficient, k_{B} the Boltzmann constant and T the temperature. The thermal fluctuating forces which the surrounding fluid exerts on the particle are modeled by zero-mean Gaussian white noise $\vec{\xi}(t)$, obeying the fluctuation–dissipation relation $\langle \xi_i(t)\, \xi_j(t') \rangle = 2\, \delta_{ij}\, \delta(t - t')$ for $i, j = x, y$. In addition to Eq. (3), the full problem is set up by imposing reflecting boundary conditions at the channel walls. For the sake of simplicity, we measure lengths by the periodicity of the channel L, time by $\tau = \gamma L^2/(k_{\mathrm{B}} T_{\mathrm{R}})$ which is the corresponding characteristic diffusion time at an arbitrary but irrelevant reference temperature T_{R}, and force by $F_{\mathrm{R}} = k_{\mathrm{B}} T_{\mathrm{R}}/L$. Consequently, the Langevin equation reads in dimensionless form:

$$\frac{d\vec{r}}{dt} = F\, \vec{e_x} + \sqrt{D}\, \vec{\xi}(t)\,, \tag{4}$$

where $D = T/T_{\mathrm{R}}$ is the dimensionless temperature, and the boundary function is given by:

$$\omega(x) = \frac{w_{\max}}{2}\, (1 - \varepsilon)\, \left\{ \sin(2\pi x) + \frac{1 + \varepsilon}{1 - \varepsilon} \right\}. \tag{5}$$

The corresponding Fokker–Planck equation for the time evolution of the probability distribution $P(\vec{r}, t)$ takes in dimensionless units the form [34,35]:

$$\frac{\partial P(\vec{r}, t)}{\partial t} = -\vec{\nabla} \cdot \left(\vec{F} - D\, \vec{\nabla} \right) P(\vec{r}, t)\,. \tag{6}$$

Since, in the present situation, we deal with irregular and impenetrable channel walls, the reflection of particles at the boundaries leads to a vanishing probability current [1]. Solving the full problem in a higher dimensional space with this irregular boundaries is a difficult task and so far there is no analytical method. Despite the inherent complexity of this problem an approximate solution can be found by introducing an effective one-dimensional kinetic description where geometric constraints and bottlenecks are considered as entropic barriers [4, 36–39].

3. The origin of entropic barriers

The dynamics of the system can be approximatively described by means of a 1D kinetic equation, obtained originally from 3D (or 2D) Smoluchowski equation by assuming fast equilibration in orthogonal channel direction. This so-called Fick–Jacobs equation reads in presence of an applied bias [4]

$$\frac{\partial P(x,t)}{\partial t} = \frac{\partial}{\partial x}\left(D(x)\frac{\partial P(x,t)}{\partial x} + \frac{D(x)}{D}\frac{\partial A(x)}{\partial x}\, P(x,t)\right) , \tag{7}$$

and approximate the full dynamics for $\omega'(x) \ll 1$. In Eq. (7), $P(x,t)$ is the probability distribution function along the length of the 3D tube or 2D channel, $A(x)$ defines the free energy:

$$A(x) := E - TS = -Fx - D\ln s(x)\,, \tag{8}$$

where $s(x)$ is the dimensionless transverse cross-section $s(x) := \pi\omega^2(x)$ in 3D, and dimension less width $s(x) := 2\omega(x)$ in 2D, where $\omega(x)$ is the radius of the pore in 3D (or the half-width of the channel in 2D). Interestingly, bottlenecks in the channel structure accounts for barriers in the potential function $A(x)$ whose height scales with the temperature indicating a clear entropic contribution. In this terms our model system allows for investigation of transport in presence of entropic barriers.

The spatially diffusion coefficient appearing in Eq. (7) reads

$$D(x) = \frac{D}{(1+\omega'(x)^2)^{\alpha}}\,, \tag{9}$$

where $\alpha = 1/3, 1/2$ for two and three dimensions, respectively. Here, introducing the spatially diffusion coefficient, into the kinetic equation, improves the accuracy, and extends its validity to more winding structures [4, 37–42].

4. Transport characteristics

For the transport of Brownian particles the quantities of interest are: the mean particle velocity $\langle \dot{x} \rangle$, respectively the nonlinear mobility $\mu = \langle \dot{x} \rangle / F$, the effective diffusion coefficient D_{eff}, and a measure for the quality of the transport. For the latter we take the so-called Q-factor, which is the ratio of the effective diffusion coefficient and the particle current, reading

$$Q = \frac{D_{\text{eff}}}{\langle \dot{x} \rangle}\,. \tag{10}$$

4.1. Analytics

After applying the equilibration assumption pointed out in Sec. 3, Eq. (7) could be derived. For periodic structures analytical expressions for the above mentioned transport characteristics can be determined by using the mean first passage time approach [4, 39, 40]. Accordingly, the average particle current is given by

$$\langle \dot{x} \rangle = \frac{1 - e^{-F/D}}{\int\limits_0^1 I(z)\, dz}\,, \tag{11}$$

and the effective diffusion coefficient by

$$D_{\text{eff}} = \frac{\int\limits_0^1 \int\limits_{x-1}^{x} \frac{D(z)\, e^{A(x)/D}}{D(x)\, e^{A(z)/D}}\, [I(z)]^2\, dx\, dz}{\left[\int\limits_0^1 I(z)\, dz\right]^3}\,, \tag{12}$$

where the integral function reads

$$I(z) = \frac{e^{A(z)/D}}{D(z)} \int\limits_{z-1}^{z} dy\, e^{-A(y)/D}\,. \tag{13}$$

In the case of an energy barrier, the driving force F and the temperature D are two independent variables, whereas for entropic transport, both current and effective diffusion are controlled by a scaling parameter F/D [1,4,39,40]. As, for a given structure, the nonlinear mobility $\mu = \langle \dot{x} \rangle / F$, the ratio of effective diffusion D_{eff} and bulk diffusion D solely depend on the scaling parameter F/D, the same applies for the Q-factor and Eq. (10) reduces to:

$$Q = \frac{D_{\text{eff}}/D}{\mu}\, Q_{\text{free}}\,, \tag{14}$$

where Q_{free} is the Q-factor for the biased Brownian motion in absence of geometrical constraints (free case) which is the inverse of the scaling parameter, *i.e.*, $Q_{\text{free}} = 1/(F/D)$.

4.2. Brownian dynamics simulations

The approximative transport characteristics described above can also be compared with those obtained from precise numerical simulations considering the full 2D dynamics. The mean particle current and the effective diffusion coefficient, have been corroborated by performing Brownian dynamic simulations by integrating the Langevin equation Eq. (3), within the stochastic Euler-algorithm. Then, the mean velocity in x-direction is given by

$$\langle \dot{x} \rangle = \lim_{t \to \infty} \frac{x(t)}{t} \,, \tag{15}$$

and the corresponding effective diffusion coefficient reads

$$D_{\text{eff}} = \lim_{t \to \infty} \frac{\langle x^2(t) \rangle - \langle x(t) \rangle^2}{2t} \,. \tag{16}$$

By comparison of the precise numerical and the analytical results for different channel geometries, the validity of the equilibration assumption could be analyzed in detail [39, 40].

5. Geometry controlled transport

The confinement by the considered channel geometry can be altered by systematically changing the parameters $w_{\max}$ and ε in the geometric function, Eq. (5). Changing these parameters we can consider two cases: *constant-ratio-scaling* and *constant-width-scaling*. In the former case, we modify the maximum width $w_{\max}$ of the geometry and keep the aspect ratio ε constant. Consequently, by applying the constant-ratio-scaling the minimum width, *i.e.* the width at the bottlenecks, is changing by modifying the maximum width. In contrast, in the constant-width-scaling, we keep the maximum width $w_{\max}$ constant and change the aspect ratio ε. In the following we analyze the transport characteristics within the two different scaling regimes.

5.1. Constant-ratio-scaling

In constant-ratio-scaling, we fix the ratio of maximum and minimum width. Hence, by increasing the maximum width $w_{\max}$ the channel is diluted in orthogonal channel direction. The advantage of this scaling is related to the effect, that within the approximative reduced dynamics, the height of the entropic barriers is kept fixed while the curvature of the effective potential at the minima and maxima varies. In Fig. 2 the mean particle current and the effective diffusion coefficient are depicted for different maximum channel widths. Strikingly, the particle current $\langle \dot{x} \rangle$ decreases with increasing effective temperature D [1, 4]. This is in contrast to the transport over

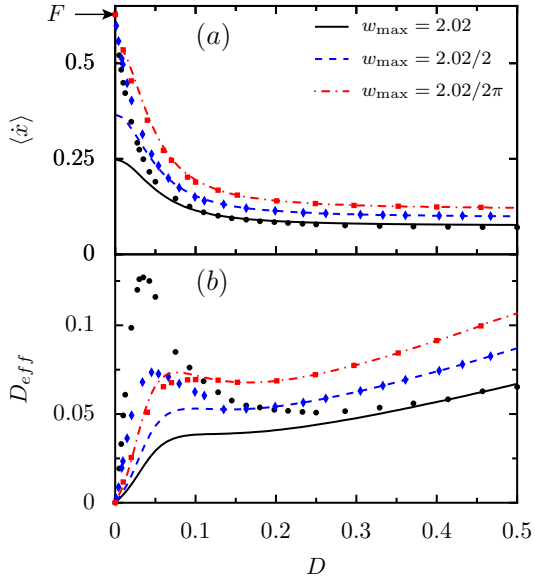

Fig. 2. (Color online.) Noise (temperature) dependence of the average particle current (a) and the effective diffusion coefficient (b) for a symmetric two-dimensional channel with the shape defined by Eq. (5) at the force value $F = 0.628$ and for various values of the maximum half-width ($w_{\max}$) of the geometry and for a constant aspect ratio $\varepsilon = 0.01$. The lines correspond to the analytic, approximative results given by Eqs. (11) and (12). The different symbols correspond to simulation results, *cf.* Eqs. (15) and (16). The arrow indicates the particle current for the deterministic limit for which the particle current equals F.

energetic potential barriers where thermal activation leads to an increasing particle current when the temperature is increased [34]. In our system, temperature dictates the height of the entropic barriers. With increasing temperature, the height of the barriers increases and the particle current decreases, *cf.* Fig. 2(a). In the deterministic limit, *i.e.*, $D \to 0$ the average particle current equals to the applied bias F irrespective of the maximum channel width. In this limit, the particles do not explore the side bags of the channel structure and move within a region defined by the width at the bottleneck. Consequently, the particles assume the velocity of a biased free particle. However, this observation is not captured by the analytics, as the influence of the winding of the structure is overestimated in the spatially dependent diffusion coefficient [40].

As the maximum width increases, the area of the size bags increases. More available space in the orthogonal channel, however, leads to reduced particle current along the channel direction. Therefore, the particle current

decreases with increasing maximum width, *cf.* Fig. 2(a). A similar reasoning applies for the increased enhancement of diffusion, which becomes visible in Fig. 2(b). The effective diffusion coefficient does not depend monotonously on the temperature D, and exhibits the effect of enhancement of diffusion [4].

Overall, for small values of $w_{\max}$, *i.e.*, smooth geometries the analytical description leads to better results whereas it fails for large $w_{\max}$ and small D range [1,39,40]. Also the applicability of the analytical description depends on the parameter we look at, *i.e.*, whether it is the average particle current (1st order) or the effective diffusion coefficient (2nd order).

5.2. Constant-width-scaling

If we keep the maximum width constant and increase the ε-value, the strength of the entropic nature of the system, *i.e.* the height of the entropic barrier in our system, is reduced. In Fig. 3 we depict the dependence of the average particle current and the effective diffusion coefficient on the noise strength. Once more, the particle current exhibits this peculiar dependence on the noise level which is characteristic for the transport over entropic

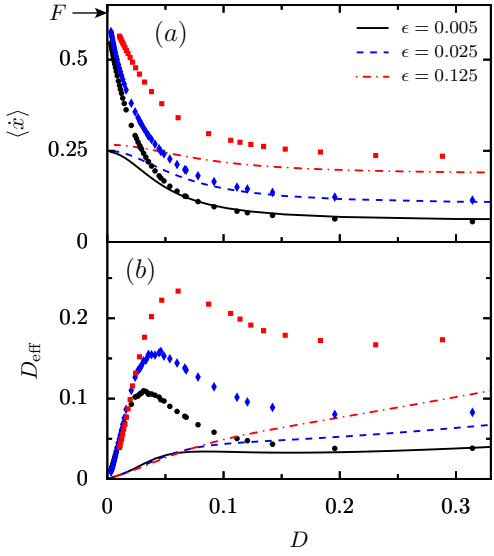

Fig. 3. (Color online.) Noise (temperature) dependence of the average particle current (a) and the effective diffusion coefficient (b) for a symmetric two-dimensional channel with the shape defined by Eq. (5) at the force value $F = 0.628$ and for various values of the aspect ratio (ε) of the geometry and for a constant maximum half-width $w_{\max} = 1$. Like in Fig. 2 lines correspond to analytic results and symbols to numerical results. Moreover, the arrow shows the particle current for the deterministic limit.

barriers. Namely, the particle current decreases with increasing noise level. In the deterministic limit, the particle current tends to the applied bias F for all values of ε, *cf.* Fig. 3(a). Upon decreasing the aspect ratio ε, the width of the bottleneck decreases and the effective height of the barrier increases. Consequently, the particle current decreases with decreasing ε.

Moreover, by decreasing the barrier height, *i.e.* increasing the ε-value, the effect of the enhancement of diffusion becomes less significant, and in the limit of a flat channel, *i.e.* for $\varepsilon \to 0$, there is linear, monotonic behavior of the effective diffusion coefficient, *cf.* Fig. 3(b).

Overall, for the constant-width-scaling, the analytical description leads to better results for the geometries with very small aspect ratio. With aspect ratio ε, the bending of the boundary function and, therefore, its derivative increases and the criteria for the applicability of the Fick–Jacobs approximation, *i.e.* $\omega'(x) \ll 1$, increasingly fails, *cf.* Fig. 3.

5.3. Comparison of the different scalings

The transport process depends on many factors such as the slope of the structure, the width of the channel at the bottleneck, the strength of the applied bias, and the thermal noise present in the system. The quality of the transport can be measured by the Q-factor which is introduced in Sec. 4. A large Q-factor means more randomness in the transport process.

Fig. 4 shows the dependence of Q for the two different scalings. Interestingly, with increasing maximum width of the channel, while keeping the aspect ratio of the channel constant, the Q-factor increases. Means, the transport becomes more noisy for larger channel widths, *cf.* the behavior of Q-factor in the inset of Fig. 4(a). The maximum of the Q-factor for wider channels is accompanied by an increased enhancement of diffusion on one side and on the other by a reduced particle current, *cf.* Sec. 5.1 and, in particular, Fig. 2.

Within the constant-width-scaling, smaller ε leads to a decrease of the height of the entropic barrier. Hence, the transport should be better in the sense of a smaller Q-factor. However, we found that for rather small and fixed values of $w_{\max}$ an increase of ε could spoil the quality of transport by increasing Q, *cf.* the behavior of the Q-factor in the inset of Fig. 4(b). Thus, by varying the aspect ratio ε of the geometry one can encounter different transport regimes. If the particular scaling parameter F/D is given, one can tune the quality of transport by choosing an optimal geometry, *i.e.*, an optimal ε-value. In addition, if the structure is given, the scaling parameter F/D may be used to control the transport. An optimal transport in the sense of a smallest Q-factor could always be achieved at either very small or very large scaling parameters F/D, *cf.* Fig. 4.

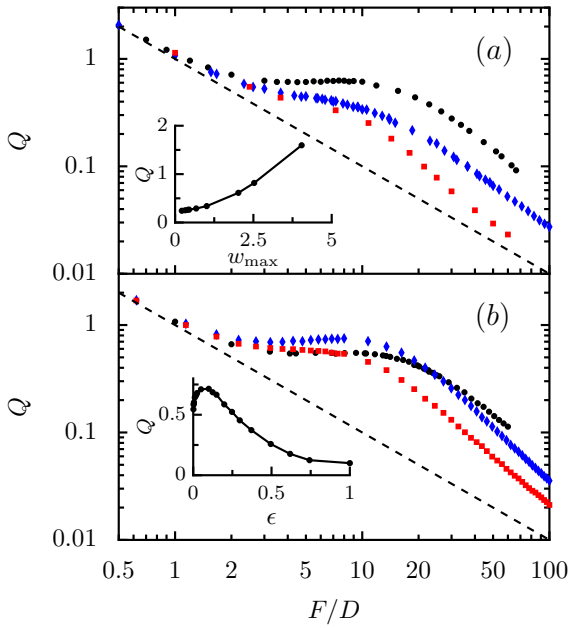

Fig. 4. (Color online.) The behavior of the Q-factor as a function of the scaling parameter F/D obtained from numerical simulations (a) for the case of constant-ratio-scaling, where the aspect ratio $\varepsilon = 0.01$, and for various values of the maximal half-width $w_{\max}$. Circles: $w_{\max} = 2.02$; triangles: $w_{\max} = 2.02/2$; squares: $w_{\max} = 2.02/2\pi$. The inset in (a) depicts the behavior of Q as a function of $w_{\max}$ at $F/D = 10$. (b) for the case of constant-width-scaling, where the maximal half-width $w_{\max} = 1$, and for various values of the aspect ratio ε. Circles: $\varepsilon = 0.001$; triangles: $\varepsilon = 0.075$; squares: $\varepsilon = 0.03$. The inset in (b) depicts the behavior of Q as a function of ε at $F/D = 10$. The dashed line in both the figures correspond to $Q_{\text{free}} = 1/(F/D)$.

6. Conclusions

In this work we analyzed the transport of Brownian particles through channels with periodically varying width, which exhibit narrow bottlenecks. The effect of confinement can be recast in terms of an entropic potential, and the dynamics of the system can be effectively described by means of the Fick–Jacobs equation with a spatially dependent diffusion coefficient. We observe peculiar transport phenomena, which are characteristic for the transport over the entropic potential barriers. The transport characteristics like the average particle current and the effective diffusion coefficient sensitively depend on the geometry of the channel. Depending on the geometric parameters we have considered two scaling regimes: the *constant-width-scaling*, for which we keep the maximum width constant, and the *constant-ratio-scaling*

where the ratio of the maximum and the minimum width of the channel is kept fixed. For the former case, the diffusion process varies upon changing the aspect ratio of the geometry. There is a critical bottleneck opening related to a maximum effective diffusion coefficient. This feature is more visible in highly confined geometries, *i.e.*, for smaller $w_{\max}$ values. In both geometric scalings, during the crossover region from a purely energetic to entropy dominated regime, optimal transport could be observed, suggesting that by increasing the noise strength D the system may exhibit better transport, *i.e.*, smaller Q-factor. Thus, tuning the parameters the aspect ratio ε, the maximal half-width $w_{\max}$ and D, one can effectively regulate the transport characteristics in these confined geometries. However, in general, controlling the width ratio ε and the maximal half-width $w_{\max}$ of the geometry may not be feasible, but, tuning the scaling parameter F/D one can arrive at an optimal transport regime.

This work was made possible thanks to the financial support by: the Max Planck Society, the Volkswagen Foundation (project I/83902); the Deutsche Forschungsgemeinschaft (DFG) via project No. 1517/26-2 and via the collaborative research center, SFB-486, project A10; the China Scholarship Council (CSC) and the Nanosystems Initiative Munich (NIM).

REFERENCES

[1] P.S. Burada, P. Hänggi, F. Marchesoni, G. Schmid, P. Talkner, *ChemPhysChem* **10**, 45 (2009).

[2] P. Reimann, C. Van den Broeck, H. Linke, P. Hänggi, J.M. Rubí, A. Pérez-Madrid, *Phys. Rev. Lett.* **87**, 010602 (2001); *Phys. Rev.* **E65**, 031104 (2002).

[3] B. Lindner, M. Kostur, L. Schimansky-Geier, *Fluct. Noise Lett.* **1**, R25 (2001).

[4] D. Reguera, G. Schmid, P.S. Burada, J.M. Rubí, P. Reimann, P. Hänggi, *Phys. Rev. Lett.* **96**, 130603 (2006).

[5] B. Hille, *Ion Channels of Excitable Membranes*, Sinauer, Sunderland 2001.

[6] L. Liu, P. Li, S.A. Asher, *Nature* **397**, 141 (1999).

[7] Z. Siwy, I.D. Kosinska, A. Fulinski, C.R. Martin, *Phys. Rev. Lett.* **94**, 048102 (2005).

[8] A.M. Berezhkovskii, S.M. Bezrukov, *Biophys. J.* **88**, L17 (2005).

[9] R.M. Barrer, *Zeolites an Clay Minerals as Sorbents and Molecular Sieves* Academic Press, London 1978.

[10] T. Chou, D. Lohse, *Phys. Rev. Lett.* **82**, 3552 (1999).

[11] C. Kettner, P. Reimann, P. Hänggi, F. Müller, *Phys. Rev.* **E61**, 312 (2000).

[12] S. Matthias, F. Müller, *Nature* **424**, 53 (2003).

[13] W.D. Volkmuth, R.H. Austin, *Nature* **358**, 600 (1992).

[14] G.I. Nixon, G.W. Slater, *J. Chem. Phys.* **117**, 4042 (2002).

[15] R. Chang, A. Yethiraj, *Phys. Rev. Lett.* **96**, 107802 (2006).

[16] I.D. Kosinska, I. Goychuk, M. Kostur, G. Schmid, P. Hänggi, *Phys. Rev.* **E77**, 031131 (2008).

[17] P. Hänggi, F. Marchesoni, *Rev. Mod. Phys.* **81**, 387 (2009).

[18] P. Hänggi, F. Marchesoni, F. Nori, *Ann. Phys. (Berlin)* **14**, 51 (2005).

[19] R.D. Astumian, P. Hänggi, *Phys. Today* **55**, 33 (2002).

[20] P. Reimann, P. Hänggi, *Appl. Phys.* **A75**, 169 (2002).

[21] U.F. Keyser, J. van der Does, C. Dekker, N.H. Dekker, *Rev. Sci. Instrum.* **77**, 105105 (2006).

[22] J. Han, H.G. Craighead, *Science* **288**, 1026 (2000).

[23] U.F. Keyser, B.N. Koeleman, S. Van Dorp, D. Krapf, R.M.M. Smeets, S.G. Lemay, N.H. Dekker, C. Dekker, *Nature Phys.* **2**, 473 (2006).

[24] A. Aksimentiev, B.J. Heng, G. Timp, K. Schulten, *Biophys. J.* **87**, 2086 (2004).

[25] J.B. Heng, C. Ho, T. Kim, R. Timp, A. Aksimentiev, Y.V. Grinkova, S. Sligar, K. Schulten, G. Timp, *Biophys. J.* **87**, 2905 (2004).

[26] J.B. Heng, A. Aksimentiev, C. Ho, P. Marks, Y.V. Grinkova, S. Sligar, K. Schulten, G. Timp, *Biophys. J.* **90**, 1098 (2006).

[27] U. Gerland, R. Bundschuh, T. Hwa, *Phys. Biol.* **1**, 19 (2004).

[28] R. Bundschuh, U. Gerland, *Phys. Rev. Lett.* **95**, 208104 (2005).

[29] I.D. Kosinska, I. Goychuk, M. Kostur, G. Schmid, P. Hänggi, *Acta Phys. Pol. B* **39**, 1137 (2008).

[30] L. Brun, M. Pastoriza-Gallego, G. Oukhaled, J. Mathé, L. Bacri, L. Auvray, J. Pelta, *Phys. Rev. Lett.* **100**, 158302 (2008).

[31] J.J. Kasianowicz, E. Brandin, D. Branton, D.W. Deamer, *Proc. Natl. Acad. Sci.* **93**, 13770 (1996).

[32] Y. Choi, A. Mecke, B.G. Orr, M.M. Banaszak Holl, J.R. Baker Jr, *Nano Lett.* **4**, 497 (2004).

[33] E.M. Purcell, *Am. J. Phys.* **45**, 3 (1977).

[34] P. Hänggi, H. Thomas, *Phys. Rep.* **88**, 207 (1982).

[35] H. Risken, *The Fokker–Planck Equation*, 2nd ed., Springer, Berlin 1989.

[36] M.H. Jacobs, *Diffusion Processes*, Springer, New York 1967.

[37] R. Zwanzig, *J. Phys. Chem.* **96**, 3926 (1992).

[38] D. Reguera, J.M. Rubi, *Phys. Rev.* **E64**, 061106 (2001).

[39] P.S. Burada, G. Schmid, D. Reguera, J.M. Rubí, P. Hänggi, *Phys. Rev.* **E75**, 051111 (2007).

[40] P.S. Burada, G. Schmid, P. Talkner, P. Hänggi, D. Reguera, J.M. Rubí, *BioSystems* **93**, 16 (2008).

[41] P. Kalinay, J.K. Percus, *Phys. Rev.* **E74**, 041203 (2006).

[42] P. Kalinay, *Phys. Rev.* **E80**, 031106 (2009).

[43] P.S. Burada, G. Schmid, P. Hänggi, *Phil. Trans. R. Soc.* **A367**, 3157 (2009).